Paper

Simulation of Anisotropic Chemical Etching of Single Crystalline Silicon using Cellular-Automata

Takamitsu Kakinaga* Student Member
Osamu Tabata* Member
Noriaki Baba* Non-member
Yoshitada Isono* Non-member
J. G. Korvink** Non-member
K. H. Ehrmann** Non-member

We propose a new concept for anisotropic single crystalline silicon (Si) etching simulation. Our approach combines three calculation modules, a molecular dynamics calculation module to define chemical reaction probability, a Cellular-Automaton module to calculate etching rate, and a Wulff-Jaccodine graphical method module to predict an etched shape. This configuration allows mm scale process simulation based on atomic scale physical chemistry of anisotropic Si etching. In this paper, the performance of a newly developed Cellular-Automata module, called CAES (Cellular-Automata Etching simulator), is presented as a first step towards the realization of our simulation concept.

Keywords: simulation, anisotropic, wet etching, silicon, molecular dynamics , Wulff-Jaccodine, Cellular-Automata

1. Introduction

Anisotropic chemical wet etching of single crystalline silicon (Si) using an alkaline solution is the standard process technology for micromachining. The importance of anisotropic Si wet etching is not impaired by the remarkable progress of dry etching technologies. However, for devices with complicated structure, mask design and etching process control become increasingly difficult. In order to reduce time and cost for prototyping, several anisotropic etching simulation methods such as a Wulff-Jaccodine method [(1)] and an atomic scale simulation method have been proposed. The simulation accuracy of the Wulff-Jaccodine method relies on the accuracy of measured etching rates for all crystallographic orientations. In order to apply this method to various etching conditions, the etching rates should be measured accurately under various etching parameters, such as the type of etchant, temperature, concentration and additives. Since this requires a lot of time and cost-consuming experiments, the available etching rate data are very limited. This constrains the utilization of the Wulff-Jaccodine method. On the other hand, a simulation technique working on surface atoms at the atomic scale can perform the simulation only using a number of removal probabilities of atoms. The simulation accuracy can be turned by changing the removal probabilities and by comparing the simulated etching rates for major crystallographic plane such as (100), (110) and (111) with those obtained from measurements. The drawbacks of this technique are: (1) it is not applicable to mm-scale simulation [(2)~(5)] because of the limitation of calculation power of current computers; (2) there are no analytical methods to determine the removal probabilities of atoms; (3) the simulation accuracy is lower than the Wulff-Jaccodine method. In order to overcome these limitations for Si anisotropic etching simulation, we propose a new concept that is composed of three calculation modules. This concept unifies: (1) the module which determines the chemical reaction probability in arbitrary etching conditions; (2) the calculation module which computes the etching rate of any crystallographic plane from the chemical reaction probability; and (3) the Wulff-Jaccodine construction method predicts the etched shape based on the etching rate of all crystallographic plane. This paper describes the outline of this concept, and the newly developed calculation module of step (2). The discussion of step (1) will be the subject of a future paper.

2. The New Concept of Anisotropic Si Etching Simulation

The outline of the new concept we proposed is shown in Fig. 1. The portions surrounded by thick lines are the three calculation

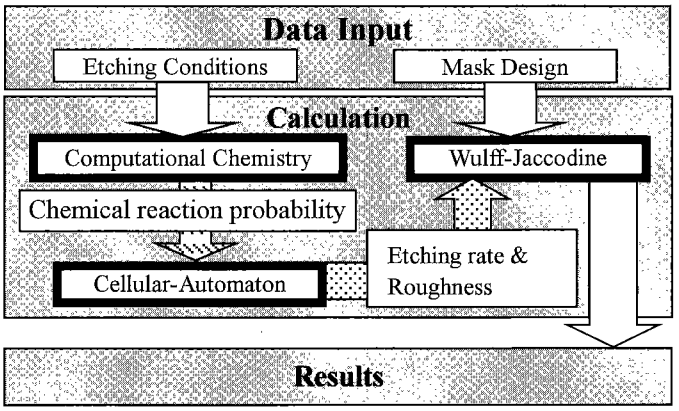

Fig. 1. The outline of our silicon anisotropic etching simulation concept.

* Ritsumeikan University
1-1-1, Noji-higashi, Kusatsu-shi, Shiga 525-8577, Japan
** University of Freiburg
Georges-Koehler-Allee, D-79110 Freiburg, Germany

modules.

A computational chemistry method calculates the chemical reaction probability according to etching conditions, i.e. by considering the configuration of surface Si atoms of the wafer, the kind of etchant, concentration, temperature, and additives used. That is, the extent to which the intensity of the back bond of a surface Si atom changes is represented as chemical reaction probability. This is because these etching conditions affect the bonding configuration of Si atoms on the surface of a wafer. Although a chemical change generally is continuous in time and space, we treat the etching reaction process in a discrete manner by stochastic transition rules in a cellular-automaton model.

The cellular-automaton (CA) model uses the reaction probability as calculated by the computational chemistry method to determine the probability of etching events. The cellular-automaton applies these probabilities to each of the surface atoms to stochastically decide which atoms to remove during a timestep. Repetition of this time step leads to surface roughness and an etching rate for the crystal plane.

Finally, the Wulff-Jaccodine is used to determine the etched 3-dimensional structure after etching by considering the mask pattern and etching rates provided by the CA which in turn is represented by etching vectors.

3. The Calculation Module Using Cellular-Automaton

The calculation module of cellular-automaton which plays the role that computes an etching rate is explained. In CAES (Cellular-Automata Etching Simulator), time and space are discrete, and the state of a system is determined by the local interaction of each element of a spatial lattice point. Therefore, calculation of CA is defined by the following steps.

Step-1 A procession with a characteristic element value is made.

Step-2 The function to make changing the value of each matrix element is defined.

Step-3 The function is made to apply to a matrix and repeat, and the value of all elements is simultaneously updated for every time step.

In the simulation of etching by CA, Step 1 corresponds to the unit lattice of a Si crystal. Intension of the situation around a cell and the state of the atom in a cell is carried out to an element value as information. The function of Step 2 is an etching rule, and the etching depth and roughness are computed by repeating update at the time step of Step 3 [4][5].

4. CAES

We developed CAES using the *Mathematica* programming language. *Mathematica* is excellent in storing various elements of different data types in large lists and provides capabilities of working on these, such as the application of a transition rule. CAES has two main purposes: (1) calculating the etching rate of each crystal plane; and (2) computing the roughness at an atomic scale. In (1), if the maximum m of a mirror index (m is a natural number) is entered, the etching rate of each plane of (hkl): $0 \leqq h, k, l \leqq m$ (h, k, and l are integers) will be calculated. For example, if $m = 2$, the etching rate of (100), (110), (111), (210), (211), and (221) will be computed. The retreat speed of the (hkl) plane indicates its etching rate.

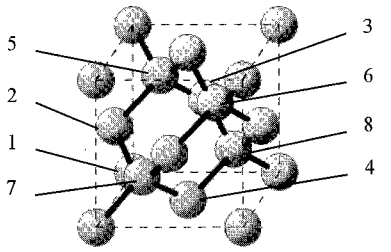

Fig. 2. A unit cell of Si. The numbered atoms constitute a unit cell.

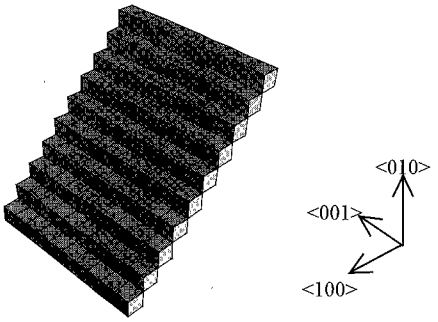

Fig. 3. The initial unit-cell surface of the (110) plane. Each unit cell is completely filled with Si atoms (see Fig. 2).

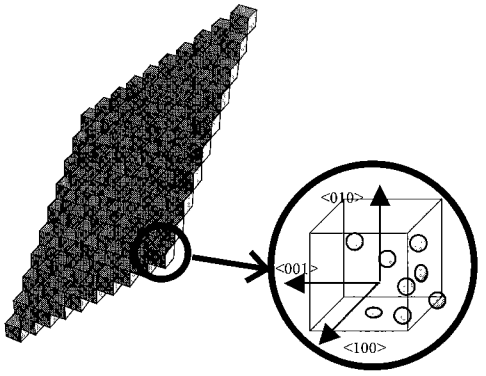

Fig. 4. The initial surface of the (111) plane. Each unit cell is completely filled with Si atoms (see insert and Fig. 2).

In CAES, the Si crystal is represented by cubic unit cells featuring (100) faces. Although the physical unit cell contains 18 atoms, from symmetry considerations, we may define a unit cell to have eight atoms as shown in Fig.2. Surface cells may loose atoms through etching until all atoms are etched away, so that eventually the empty unit cell may be removed from the data structure.

Prior to the simulation, unit cells are initialized along the (hkl) plane as specified. Figure 3 and 4 show the cell array for (110) and (111) planes, respectively, after initialization.

In order to obtain the stabilizing etching rates for calculation of the higher order plane etching rates, many time steps are needed. The etching depth in a certain plane is determined by the number of unit cells removed plus the height of the removed atoms in the surface cell. For example, if five atoms remain in the unit cell, its height is calculated to 5 / 8 of a cell height.

It is important to obtain the surface roughness in an atomic order to elucidate an etching mechanism. Moreover, surface roughness is important not only for comprehension of the mechanism but also from the application viewpoint because it is a

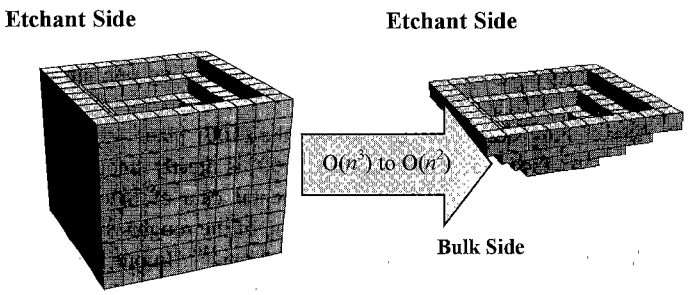

Fig. 5. The models of cells that should be modified.

quantity which determines the optical characteristics and the mechanical strength of the etched structures. In CAES, roughness is defined by the "maximum peak valley distance", which is measured at the atomic scale.

A special feature of CAES is restricting the object of updating so as to obtain a shorter calculation time. Since the transition function only removes atoms at the surface, CAES stores only the surface plus a unit-cell-deep neighborhood. Thus CAES reduces the complexity from O(n^3) to O(n^2), or from the volume to the surface. Here, n is the simulation domain size (measured in the number of unit cells) along one dimension and O(n^x) denotes that memory and time consumption scale proportional to n^x. During matrix assembly, only the cells which have an atom marked as "exposed to etchant" are included. Between update cycles, new cells are taken into the matrix such that every atom exposed to the etchant has neighbors inside the crystal as shown in Fig.5.

5. Removal Probability in CAES

To start off the CAES development process, we have used the same set of removal probabilities and etching rules as is reported by Than et al. [6]. We believe that these values can be improved upon by a computational chemistry approach as indicated by step (1), which we will address in a future publication. The removal probability to apply depends on the atom's constellation with respect to its neighbor configuration. Here, an atom is classified into one of three patterns. We assume the case that the atom in question for removal has only two neighbor atoms beneath the crystal surface. Then it is categorized as CASE A as shown in Fig.6a. CASE B, shown in Fig.6b, is applied for atoms with one bulk and two surface neighbors or with two bulks and one surface neighbor. Fig.6c finally shows CASE C, where a surface atom adjoins three bulk atoms. Therefore, its removal corresponds to the breaking of three bonds. On the other hand, for CASE B, the surface atom has three neighbors but one or two of the neighbors are exposed to etchant as an atom for removal.

Therefore, the bond of the atom for removal of CASE B is weaker than the atom for removal of CASE C.

Based on the situation described above, the removal probability of a surface atom is classified as follows:

i) an atom with two neighbor atoms;
ii) an atom with three neighbor atoms, among which at least one is a surface atom;
iii) an atom with three neighbor atoms and all three atoms are in a bulk state;
iv) the surface atom fulfills neither of the conditions of i), ii), and iii).

Removal probabilities for i), ii), and iii) are named as $p(100)$, $p(110)$ and $p(111)$, respectively, because these cases almost correspond to atoms for the (100), (110) and (111) planes. The removal probability $p(hkl)$ for the (hkl) plane is defined with its corresponding etching rate $r(hkl)$ by

$$p(hkl) = r(hkl) / r_{\max} \quad \cdots\cdots (1)$$

with $0 \leqq p(hkl) \leqq 1$ and the etching rate $r(hkl)$ ($h, k, l = 0$ or 1) and $r_{\max}$ being the maximum of $r(100)$, $r(110)$, $r(111)$. As an exception, the removal probability for iv) is the as same as for CASE B.

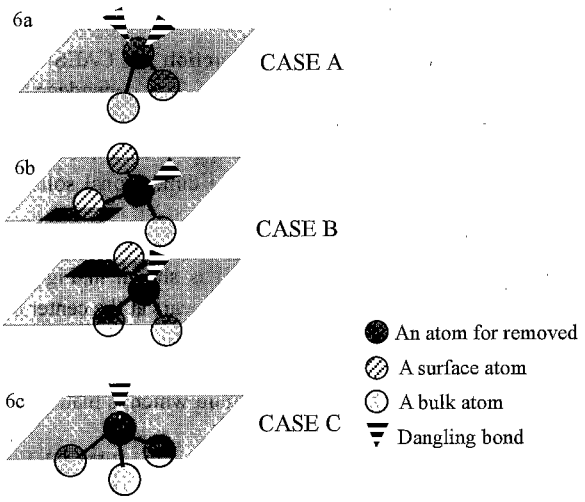

Fig. 6. The categories of surface atom.

6. Etching Rule

Whether an atom is etched or not is determined by considering a random number assigned to the surface atom. If the random number is bigger than the removal probability, the surface atom is not removed. Therefore, supposing the removal probability of the n-th atom for removal is p_n and the assigned random number is e_n ($0 \leqq e \leqq 1$):

If $p_n \geqq e_n$, the atom is removed;
If $p_n < e_n$, the atom is not removed.

Combined with the removal probabilities as introduced, we may specify the etching rule as:

a) In the case of i), if a random number e is within [0, $p(100)$], the Si atom is removed;
b) In the case of ii), if a random number e is within [0, $p(110)$] , the Si atom is removed;
c) In the case of iii), if a random number e is within [0, $p(111)$] , the Si atom is removed;
d) In the case of iv), d1) the Si atom will not be etched if it is a bulk atom, d2) or, the Si atom will be etched if the atom is on the surface.

In previous work, the removal probability of Eq.(1), the calculated etching rate ratio of each plane did not coincide with the entered p_n value [7]. In order to verify how much the etching rate depends on the removal probability, a simulation run with squared removal probability was also performed. Namely, Eq.(1) changes to:

$$p(hkl) = \{r(hkl) / r_{\max}\}^2 \quad \cdots\cdots (2)$$

7. Verification of Operation and Discussion

7.1 Graphics and a Display Function CAES visualizes its simulation results in different ways. The dependency of the etching rate on the crystallographic planes is visualized through a stereographic projection as shown in Fig.7, while the advance of etching process is expressed by a three dimensional solid figures and a contour lines as shown in Fig.8.

A structure etched through a square window mask aligned to the <100> directions of (100) oriented Si is shown in Fig.8. These Figs show the large scale of under cut appears at the center of each line. At the beginning of etching, the etched structure was not inverted pyramid due to the atomic scale roughness. This under cut eventually forms an inverted pyramid which is made by {111} planes.

7.2 Time Dependence of Etching Rate and Roughness

In order to check the basic functionality of CAES, we observed the progress of the etching depth and roughness in time. Results are shown in Fig.9 and Fig.10, respectively. These results were calculated using probabilities from Eq.(2). The cell size of 20x20 was used for the calculation. In advance, it was checked that 20x20 cells are enough to have small-dispersed calculated data.

In the case of (111) plane, etching advances in a stepwise manner as shown in Fig.9, and roughness curve shows rectangular parts as shown in Fig.10. In order to clarify the reason of these behavior of (111) plane, the simulated etching process was observed in atomic scale. From the observation, it was concluded that these results show the (111) surface in 20x20 cells is etched "layer-by-layer". The step value of 0.32 nm is identical with the thickness of one layer. This result agrees the experimental observation [8].

The etching depth against time plot of the (110) plane is almost linear as shown in Fig.9. However, the etching rate obtained by differentiating the time plot becomes gradually large as shown in Fig.11. While, the (110) plane's roughness also increased with time as shown in Fig.10. Therefore, these results suggest a kind of relation is existing between roughness and increasing rate during etching.

The etching depth against time of the (100) plane advanced linearly and the surface roughness of (100) is mostly stable. This simulations result agrees with experimental data of Sato *et al.* They reported in their study that the value of the roughness of the (100) plane was constant and was about 2 nm [10]. In our work, a surface roughness of the (100) plane was constant at a value of 0.54 nm.

7.3 Surface Morphology of the (111) Plane It is reported that μm-scale geometric patterns appeared on the etched surface of (111) plane [10]-[12]. At the μm scale, Masuda *et al.* reported that the etched surface of the (111) plane with TMAH was covered with hexagonal wrinkles of various sizes in the early stage of the etching [11]. On the other hand, according to the report of Veenendaal *et al.*, when a Si (111) surface is etched in KOH, triangularly shaped etch-pits were observed [12]. The triangle is

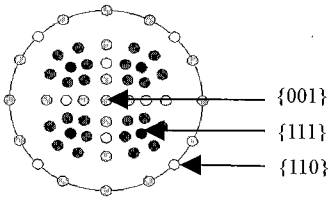

Fig. 7. A stereographic projection of the etching rate. Light and dark marks denote high and low etching rate, respectively.

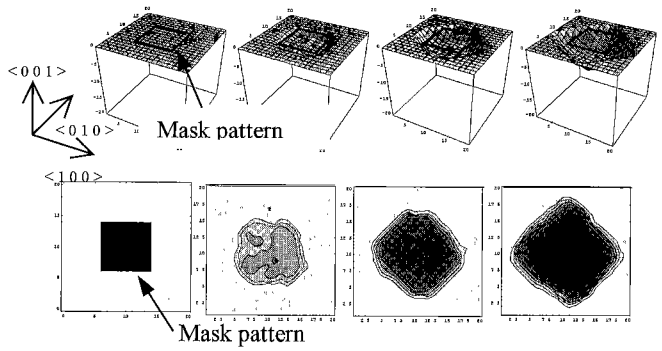

Fig. 8. The 3-D figure and the contour map of etching of a square pattern aligned to <100> direction.

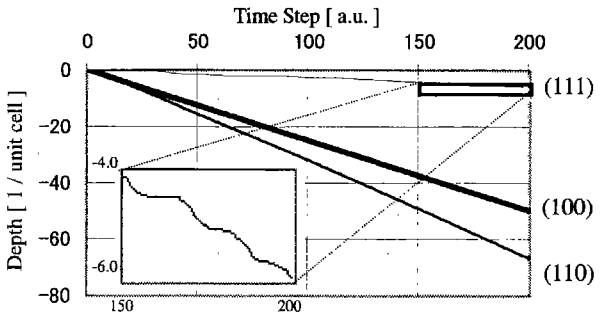

Fig. 9. Etching depth vs. simulation time. 20x20 cells and 200 time steps.

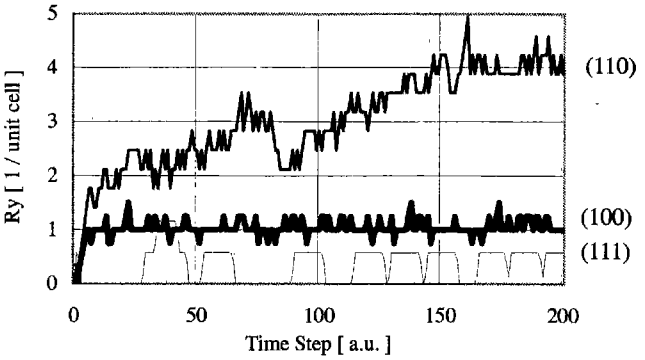

Fig. 10. Change of roughness vs. simulation time.

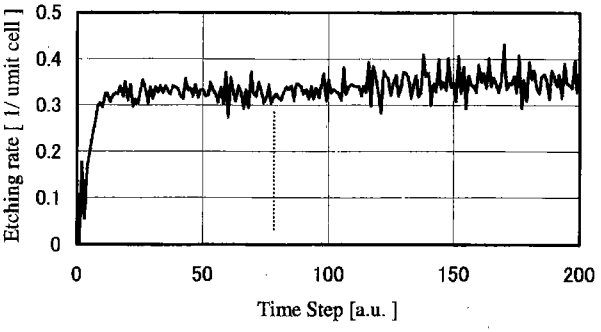

Fig. 11. Etching rate of the (110) plane vs. time.

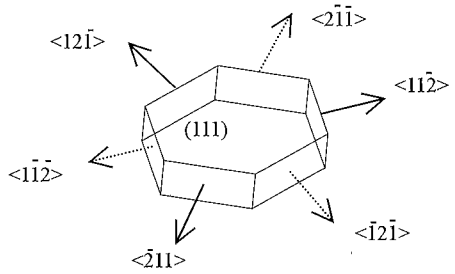

Fig. 12. Hexagonal shape surrounded by the $\{11\bar{2}\}$ planes on the (111) plane.

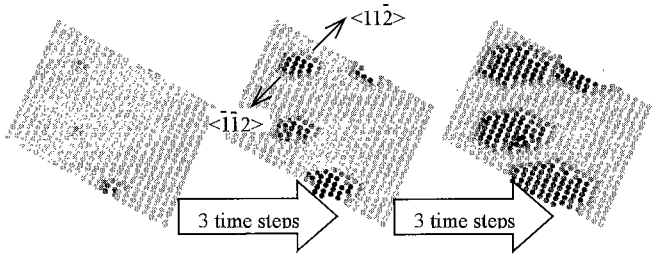

Fig. 13. Etched surfaces of the (111) plane.

formed by $\{11\bar{2}\}$ lines. Furthermore, Sato *et al.* reported that when (111) was etched with two different etchants, KOH and TMAH, the etch-pits were quite different by the two etchants in μm scale [13]. According to their reports, this difference of etch-pits shape was resulted from the difference of the ratio of the step velocities aligned to $<11\bar{2}>$ and $<\bar{1}\,\bar{1}2>$ as shown in Fig.12. The sides that are etched faster than the other sides diminish little by little. These phenomena on (111) plane have been observed in μm-scale. However, since the μm-scale phenomena are caused by the arrangement of the atoms, it is expected that the similar geometric patterns of atomic-scale is observed.

CAES stores the locations of all atoms during etching simulation on each time plots, so etching process of the (111) plane is visualized in atomic scale. It is expected that the difference of the step velocities are explained by the difference of the removal probabilities in CAES. In our work, on the surface of the (111) plane, atomic-scale hexagonal shapes were observed as shown in Fig.13. Here, Eq.(2) is applied to the removal probability. The lines which compose the hexagonal shape correspond with the directions shown in Fig.12. Each atom that makes the sides is shown in Fig.14. Here, the removal probabilities of the atoms are symbolized as $P(xy)$ by the number of neighbor atom x and bulk atom y in neighbor atoms. As shown in Fig.14, three types of atoms appear on the lines and the removal probabilities of three types of atoms are not same. In spite of $P(21)$ has small value than unity, etching proceeds at same step velocity for every directions. The reason is as follows; $P(21)$-atoms appeared is connected with $P(32)$-atoms as shown in Fig.14. Since $P(32)$ equals unity, $P(21)$-atoms always removed with $P(32)$-atoms.

In order to verify the possibility to simulate the different geographic pattern appeared on TMAH and KOH, simulation was carried out with changing the removal probability. If $P(31)$ is smaller than $P(32)$, etching step of the direction of $<11\bar{2}>$ became faster than $<\bar{1}\,\bar{1}2>$ as shown in Fig.15-(a). Oppositely, when $P(32)$ is smaller than $P(31)$, etching velocity of $<\bar{1}\,\bar{1}2>$ become faster than $<11\bar{2}>$ as shown in Fig.15-(b). Where, the apexes that

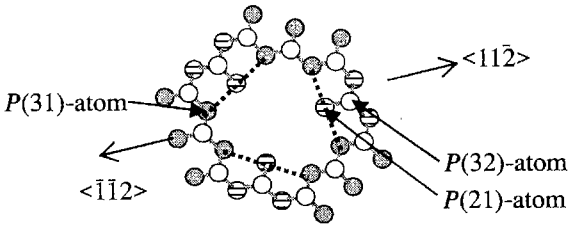

Directions	Neighbor atoms	Bulk atoms	Surface atoms	Removal probabilities by Eq(2)
$<11\bar{2}>$	3	2	1	$P(32)=1$
	2	1	1	$P(21)=0.36$
$<\bar{1}\,\bar{1}2>$	3	1	2	$P(31)=1$

Fig. 14. States of the atoms that appear when the (111) plane is etched.

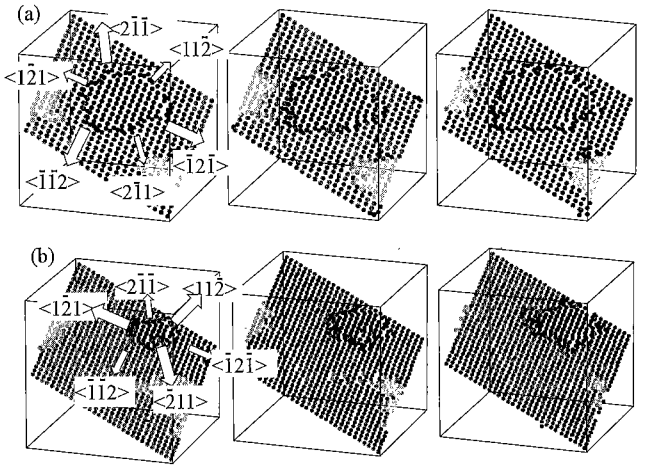

(a); $P(32)=0.8, P(31)=0.1$,
(b); $P(32)=0.1, P(31)=1$

Fig. 15. Etched surfaces of the (111) plane. Round brackets show time step.

make hexagonal morphology are controlled by $P(32)$. Therefore, if $P(32)$ equals unity, hexagonal shapes remain. Because of this reason, in order realize the triangular shape appeared in KOH etching, the removal probability of $P(32)$ in Fig.15-(a) has to be less than 1. From these results, it was confirmed that this simulator is possible to show the difference of the atomic scale geometric pattern between KOH and TMAH just changing the removal probability without changing the etching rule.

7.4 Removal Probability Dependence of the Etching Rate

We investigated how removal probabilities affect etching rates. Table 1. shows the etching rates obtained using probabilities from Eq.(1) and Eq.(2).

Eq.(1) and (2) provide ratios of the etching rate (111)/(100) of 0.592 and 0.128, respectively. As it was already shown for the etching process of a (111) plane, etching proceeds so that a skin is stripped from the surface. Therefore, the etching rate of the (111) plane depends on the probability of appearance of a vacancy, namely, the removal probability of $p(111)$ in this case, and the step velocity of the lines. However, the spreading velocity of the

Table 1. The etching rate obtained using Eq. (1) and (2).

crystallographic planes		(100)	(110)	(111)
Initial input rate		$P(110)=30$	$P(100)=50$	$P(111)=1$
Equation (1)	Obtained etching rate ratio for (100)	1.000	1.340	0.592
Equation (2)	Obtained etching rate ratio for (100)	1.000	1.256	0.128

wrinkles is not so strongly affected by $p(111)$ because $p(100)$ (CASE A) and $p(110)$ (CASE B) is applied during the stripping of a monolayer. Since $p(111)$ is much lower than $p(100)$ and $p(110)$, it is thought that the etching rate of the (111) plane is dominated by $p(111)$. Therefore, the etching rate of the (111) plane was influenced by decreasing the removal probability of $p(111)$ from 1/50 from Eq.(1) to 1/2500 from Eq.(2). However, the simulated etching rate ratio of 0.128 is still larger than both the experimental data ratio of (111)/(100) of 0.033 for TMAH at 90 °C (22wt%) and of 2.5 x 10^{-3} for KOH at 92 °C (20wt%) [11]. If the much lower removal probability of $p(111)$ is adopted, the closer the simulated results matched the experimental values.

8. Conclusions

- A new concept, aiming to be more useful for industry and at the elucidation of an etching process, was proposed. In the concept, we developed and verified a simulator named CAES that simulates the directional etching rate.
- CAES, a wet silicon etching simulator based on a cellular automaton with a stochastic rule set, was developed. It is tailored to eventually take the place of an etching rate server within our new concept of an etching simulation toolkit.
- Etching processes, during etching on (111) plane in atomic scale, were observed. From these results, it was confirmed that CAES shows the difference of the atomic scale geometric pattern between KOH and TMAH just changing the removal probability without changing the etching rule.

In this work, it was concluded that CAES can calculate the behavior of etching rates and surface roughness for an extended time step because of the updating feature. In the next research step, we will calculate the etching rate and surface roughness about a larger set of high order planes with extended time steps and conduct the surface morphology observation with an AFM to compare simulated results with experimental data.

(Manuscript received Mar. 20, 2003, revised Sep. 3. 2003)

References

(1) J. Fruehauf, et al. . "A simulation tool for orientation dependent etchng", *J. Micromech. Microeng.*, 3, pp 113-115 (1993)

(2) H. Camon, et al : "New trends in atomic scale simulation of wet chemical etching of silicon with KOH", *Materials Scince and Engineering*, B37, pp.142-145 (1996)

(3) M. A. Gosalvez, et al. : "Anisotropic wet chemical etching of crystalline silicon: atomistic Monte-Carlo simulations and experiments", *Appl. Surface Scince*, 178, pp.7-26 (2001)

(4) Z. Mokatadirt and H. Camon : "Monte carlo simulation of anisotropic etching of silicon: investigation of <111> surface properties", Modelling Simul Mater. Sci. Eng., 5, pp.481-488 (1997)

(5) F. H. Stillinger and T. A. Weber : "Computer simulation of local order in condensed phases of silicon", *Physical Review B*, Vol 31, No.8, 15 April (1985)

(6) O Than and S. Buettgenbach : "Simulation of anisotropic chemical etching of crystalline silicon using a cellular automata model", *Sensors and Actuators* A 45, pp 85-89 (1994)

(7) T. Kakinaga, et al. : 3rd Workshop on Physical Chemistry of Wet Etching of Silicon, pp.43-46 (2002)

(8) P. Allongue; V Costa-Kieling; H. Gerischer : "*Etching of NaOH Solutions*", J of Electrochem. Soc. 140, pp 1009- 1026 (1993)

(9) M. Shikida, et al. : "Comparison of Anisotropic Etching Properties between KOH and TMAH Solutions", Proc of IEEE Int. MEMS-99 Conf., pp 315-320 (Orlando, 17 21. Jan. 1999)

(10) Z. Moktadir and K. Sato : "Wavelet charactarization of the submicron surfaceroughness of anisotropically etched silicon", Surface Scine Letters, 2751, 01-6 27 October (2000)

(11) T Masuda, et al. : "Surface roughness of single-crystal silicon etched by TMAH solution", Technical Digest of the 17th Sensor Symposium, pp.263-266 (2000)

(12) E. van Veenendaal, K. Sato, M. Shikida, and J van Suchtelen : "Micromorphology of single crystalline silicon surfaces during anisotropic wet chemical etching in KOH and TMAH", *Sensours and Actuators* A 93, pp.219-231 (2001)

(13) K. Sato, T. Masuda, and M Shikida : 3rd Workshop on Physical Chemistry of Wet Etching of Silicon, pp.43-46 (2002)

Takamitsu Kakinaga (Student Member) He received the M.S. degree in 1998, in the department of physics from Kyushu University, Fukuoka, Japan. Since 1998, he has been with the Minolta Inc., Osaka, Japan. He is now a doctoral course student in the Ritsumeikan University, Shiga, Japan.

Osamu Tabata (Member) He received a M.S. degree and the Ph.D. degree from Nagoya Institute of Technology, Nagoya, Japan, in 1981 and in 1993, respectively. Since 1981, he has been with the Toyoya Central Reserch and Development Laboratories, Inc., Aichi, Japan. In1996, he joined the Department of Mechanical Engineering, Ritsumeikan University, Shiga, Japan. He is currently engaged in the research of micro/nano process, LIGA process, thin film mechanical property evaluation and MEMS. He is an associate editor of Journal of Micro Electro Mechanical Systems and an editorial board member of Sensors and Actuators. Also he is a program committee member of many International Conferences. He was honored with the Scince News Award for research in 1992, R&D 100 Award for research in 1993 and 1998. He is a member of the Institute of Electrical Engineers and the Institute of Electrical and Electronics Engineers.

Noriaki Baba (Non-member) He received the B.S. degree in 2002, in Mechanical Engineering from Ritsumeikan University. He is now a master course student in the same university.

Yoshitada Isono (Non-member) He received the M.S. degree and the Ph.D. degree from Ritsumeikan University, Kyoto, Japan, in 1991 and in 1998, respectively. Since 1991, he has been with the Mitsubishi Heavy Industry, Inc., Kyoto, Japan. In 1993, he joined the Department of Mechanical Engineering, Ritsumeikan University, Shiga, Japan. Since 1999, he has been an Associate Prof. of the Department of Mechanical Engineering and director of Micro/Nano Mechanics Laboratory. His research interests are micro/nanoscale material mechanics including the development of micro/nanotesting technology for the design of MEMS/NEMS. He is currently engaged in works of micro/nanotesting of MEMS materials using SPM, development of silicon nanolithography technique and development of the MEMS/NEMS devices used for micro sensors and micro bio-tools.

Jan G. Korvink (Non-member) Dr. Korvink holds the chair of microsystem simulation at the University of Freiburg. He received his D.Sc. from the Swiss Federal Institute of Technology (ETH) in 1993, and his M.Sc. from the University of Cape Town in 1987. Dr. Korvink was senior scientist at the Physical Electronics Laboratory of the ETH before moving to Freiburg. He is co-author of more than 100 technical articles in conference proceedings and journals, and has co-authored one book chapter and the SOLIDIS microsystem simulation software. He serves on the program selection committees of numerous MEMS conferences. Dr Korvink is the associate editor (Europe) for "Sensors and Materials", MYUKK, Tokyo, Japan, and of the Journal Applied Micro and Nano Technology. He is a member of the IEEE and the ASME. His main research interests are in the modelling and numerical simulation of microsystems, and in low cost polymer fabrication technology.

Klaus Heinrich Ehrmann (Non-member) He was born in Crailsheim, Germany on July 5, 1976. He received his master degree in microsystem engineering from the University of Freiburg / IMTEK in 2002, doing his thesis on a silicon gyroscope at IMEGO Göteborg. Since October 2002 he is working towards a Ph.D. degree at the EPF Lausanne on the field of micro NMR probes.